Available online at www.sciencedirect.com

ScienceDirect

Nuclear Physics A 967 (2017) 528–531

www.elsevier.com/locate/nuclphysa

Exploring jet substructure with jet shapes in ALICE

D. Caffarri for the ALICE Collaboration

CERN, Geneva, Switzerland

Abstract

The characterisation of the jet substructure can give insight into the microscopic nature of the modification induced on high-momentum partons by the Quark-Gluon Plasma that is formed in ultra-relativistic heavy-ion collisions. This modification of parton-to-jet fragmentation and of the parton virtuality, induced by the QGP, can be studied using jet shapes, in particular using jet energy redistribution, intra-jet broadening or collimation. Results of a selected set of jet shapes are presented for p–Pb collisions at $\sqrt{s_{\rm NN}}$ = 5.02 TeV and for Pb–Pb collisions at $\sqrt{s_{\rm NN}}$ = 2.76 TeV. Results are also compared with PYTHIA Perugia 11 calculations and models that include in-medium energy loss.

Keywords: jets, jet quenching, jet substructure

1. Introduction

The deconfined, highly dense and hot state of nuclear matter created in Pb–Pb collisions, known as Quark-Gluon Plasma, is expected to induce an energy loss of incoming high-momentum partons, via gluon emission. This in-medium energy loss modifies the jet yields, the parton-to-jet fragmentation and the parton virtuality, with respect to pp collisions. The measurement of such modifications brings insight into the mechanisms of energy loss of partons traversing the medium as well as the possibility to measure the parameters of the medium itself. Measurements of the same observables in p–Pb collisions allow to study possible cold nuclear matter effects that might affect the high-$p_{\rm T}$ particle production and, together with the measurements in pp collisions, provide a reference for Pb–Pb collisions.

Jet shapes are theoretically well defined observables that allow to study modifications of the fragmentation and virtuality, exploiting informations on how constituents are distributed in a jet or considering the clustering history of jets [1, 2]. A selection of jet shapes will be described in this work to probe different aspects of the possible modifications: the momentum dispersion ($p_{\rm T}^{\rm D}$), the radial moment (g) [1], the jet mass ($M_{\rm jet}$) and the shared momentum fraction (z_g).

The momentum dispersion ($p_{\rm T}^{\rm D}$) defined in Eq. 1 (left), quantifies the parton momentum redistribution into jet constituents: jets with fewer and harder constituents have higher $p_{\rm T}^{\rm D}$. The radial moment (g), defined in Eq. 1 (center-left), measures the jet constituents momentum redistribution, weighted by their distance from the jet axis in the $\eta - \varphi$ plane (ΔR_i). This shape is sensitive to the collimation or broadening of the jet[1].

[1] In these definitions, $p_{\rm T,i}$ refers to the transverse momentum of the constituents of the jets.

http://dx.doi.org/10.1016/j.nuclphysa.2017.05.007

Due to the subsequent interactions of the incoming high-p_{T} parton with other partons of the medium, an increase of its virtuality is expected. This effect would be observed as an increase of the mass of the jets, once the parton fragmented [3]. The jet mass is defined as the difference between the energy of the jet (E_{jet}) and its transverse ($p_{\mathrm{T,jet}}$) and longitudinal ($p_{\mathrm{z,jet}}$) momentum, as shown in Eq. 1 (center-right).

$$p_{\mathrm{T}}^{\mathrm{D}} = \frac{\sqrt{\sum_i p_{\mathrm{T,i}}^2}}{\sum_i p_{\mathrm{T,i}}}, \qquad g = \sum_i \frac{p_{\mathrm{T,i}}}{p_{\mathrm{T,jet}}} |\Delta R_i|, \qquad M_{\mathrm{jet}} = \sqrt{E_{\mathrm{jet}}^2 - p_{\mathrm{T,jet}}^2 - p_{\mathrm{z,jet}}^2}, \qquad z_g = \frac{\min(\mathrm{p_{T,1}}, \mathrm{p_{T,2}})}{(p_{\mathrm{T,1}} + p_{\mathrm{T,2}})}. \tag{1}$$

The momentum distribution between the two hardest subjets is also considered z_g, Eq. 1 (right), where $p_{\mathrm{T,1,2}}$ indicate the momentum of the two hardest subjets [4]. In order to find the these two branches, the soft radiation is removed from the leading partonic component of the jet, using the jet grooming algorithms [5, 6]. The measurement of the hardest subjets allows to probe the role of coherent and de-coherent emitters within one jet in the medium.

For the characterisation of the jet substructure, ALICE focuses on the low-intermediate transverse momentum ($40 < p_{\mathrm{T,jet}} < 120$ GeV/c), where stronger quenching effects are expected but also a larger background due to soft particle production is present.

2. Jet reconstruction and corrections

For the Pb–Pb analyses, the 0-10% most central collisions were selected in a sample of data collected during the 2011 LHC Run at $\sqrt{s_{NN}} = 2.76$ TeV. The p–Pb analyses, instead, were performed at $\sqrt{s_{NN}} = 5.02$ TeV exploiting a minimum bias and a jet-triggered sample, that was obtained using the ElectroMagnetic CALorimeter (EMCAL), in order to extend the momentum coverage of the measurement up to particle level jet with $p_{\mathrm{T,jet}} = 120$ GeV/c. Measurements in pp collisions have also been performed at $\sqrt{s} = 2.76$ and 7 TeV and compared with Monte Carlo generators [7].

In ALICE, jets are reconstructed using the FastJet anti-k_T algorithm with a resolution parameter $R = 0.2$ for the analysis of $p_{\mathrm{T}}^{\mathrm{D}}$ and g and $R = 0.4$ for the jet mass and z_g analyses. The E-scheme is used for the recombination and only the charged constituents in $|\eta| < 0.9$ with $p_{\mathrm{T}} > 150$ MeV/c are used to reconstruct jets, in order to exploit the maximum ALICE acceptance in the central rapidity region.

For Pb–Pb collisions an event-by-event estimate of the underlying event momentum and mass densities ρ and ρ_m respectively is performed using the area-median method, implemented in the FastJet algorithm [8]. This average background subtraction is then applied to the jet shapes, via two different methods: the area derivatives methods [9] and the constituent subtraction method [10].

In p–Pb collisions, the overall background contribution is significantly smaller than in Pb–Pb ones but its fluctuations increase due to event-by-event multiplicity fluctuations. For p–Pb analyses, then, the background was subtracted on average using unfolding techniques [11].

Residual background fluctuations and detector effects are corrected using Bayesian two-dimensional unfolding procedure, in order to obtain fully corrected, particle level jet shapes. The procedure uses the RooUnfold package [12], using a 4D response matrix that takes into account the $p_{\mathrm{T,jet}}$ and shape at particle and reconstructed levels. For Pb–Pb collisions, this response matrix is build considering the matching between particle level jets and those obtained once embedded in Pb–Pb events, after subtracting the estimated average background. For p–Pb collisions, istead, the response matrix is obtained embedding four-momentum vectors into p–Pb events, in order not to bias the multiplicity of the event.

3. Results

3.1. Results in p–Pb collisions

Fig. 1 (top) shows the results of the fully corrected jet mass distributions measured in p–Pb collisions at $\sqrt{s_{\mathrm{NN}}} = 5.02$ TeV in three bins of jet transverse momentum between 60 and 120 GeV/c [11]. The measurement is compared with PYTHIA Perugia 11 [13] and HERWIG [14] Monte Carlo simulations. An

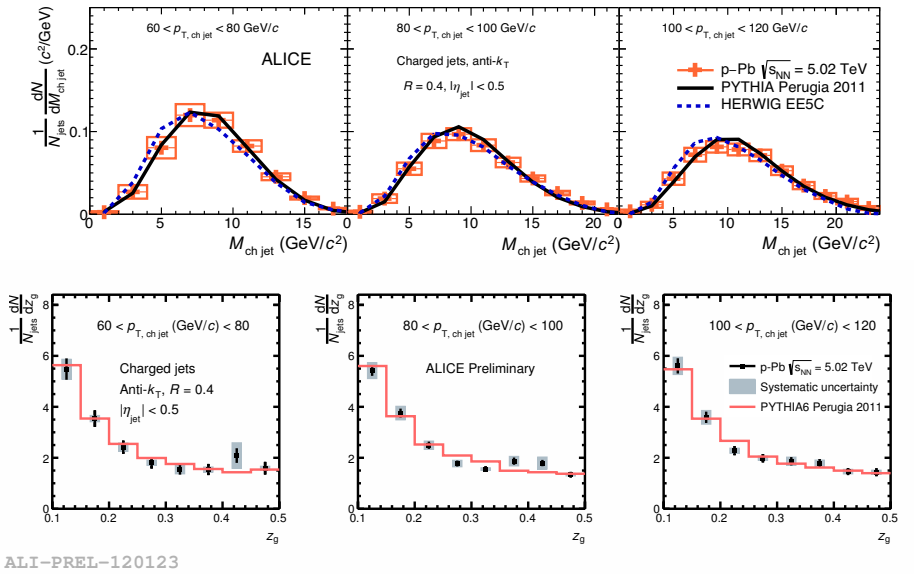

Fig. 1. Fully corrected jet mass (top) and z_g (bottom) distributions for anti-k_T jets with $R = 0.4$ and $60 < p_{T,jet} < 120$ GeV/c in p–Pb collisions $\sqrt{s_{NN}} = 5.02$ TeV, compared with PYTHIA Perugia 11 and HERWIG simulations.

agreement within 10-20% is found between data and PYTHIA Perugia 11, that worsten in the tail of the distribution. Worse agreement with HERWIG is found, in particular in the low mass tail.

Fig. 1 (bottom) shows the results of the shared momentum fraction measured in p–Pb collisions at $\sqrt{s_{NN}} = 5.02$ TeV in three bins of jet transverse momentum between 60 and 120 GeV/c. The measurement is compared with PYTHIA Perugia 11 and a good agreement is found. Both these jet shapes measurements in p–Pb collisions can be used as reference measurements for Pb–Pb.

3.2. Results in Pb–Pb collisions

Fig. 2 shows the results of the fully corrected jet mass distributions measured in Pb–Pb collisions at $\sqrt{s_{NN}} = 2.76$ TeV in three bins of $p_{T,jet}$ between 60 and 120 GeV/c [11]. This measurement shows a hint of a shift towards smaller jet mass values with respect to the p–Pb case for $p_T < 100$ GeV/c. In order to take into account the different quark and gluon composition, the different $\sqrt{s}$ in the two collision systems and the different shape in the underlying jet-p_T spectrum, a ratio of the jet mass distributions is considered and compared with PYTHIA Perugia 11 at the two energies. A hint of difference is observed also between the two ratios. A 1σ difference is observed when considering the mean jet mass for $60 < p_{T,jet} < 80$ GeV/c.

Fig. 2 shows also the comparison of the measurements with different theoretical model calculations. Data lie between PYTHIA Perugia 11 and JEWEL [15] in the case when recoil partons do not contribute to the final state hadrons. Q-PYTHIA [16] and JEWEL, when including the recoil process, predict a too large jet masses.

Fig. 3 shows fully corrected p_T^D (left) and g (right) distribution, measured in Pb–Pb collisions at $\sqrt{s_{NN}} = 2.76$ TeV for jets with $40 < p_{T,jet} < 60$ GeV/c. Results are compared with PYTHIA Perugia 11. The momentum dispersion distribution is shifted to higher values in the Pb–Pb measurement with respect to the pp Monte Carlo. The radial moment distribution is shifted to lower values in Pb–Pb collisions with respect to PYTHIA Perugia 11. In Fig. 3, results are also compared with JEWEL with both options of medium-jet recoil interaction and they are better described in the case when this option is switched off. The underlying

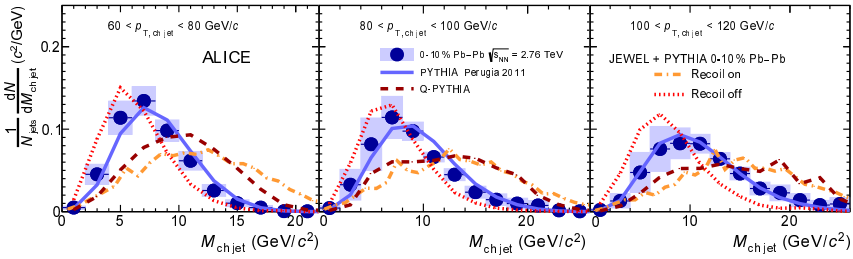

Fig. 2. Fully corrected jet mass distribution for anti-k_T jets with $R = 0.4$ and $60 < p_{T,jet} < 120$ GeV/c in Pb–Pb collisions $\sqrt{s_{NN}} = 2.76$ TeV, compared with PYTHIA Perugia 11, Q-PYTHIA and JEWEL models.

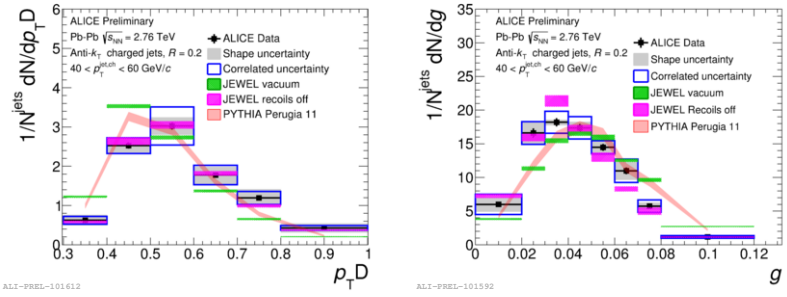

Fig. 3. Fully corrected p_T^D (left) and g (right) distributions for anti-k_T jets with $R = 0.2$ and $40 < p_{T,jet} < 60$ GeV/c in Pb–Pb collisions at $\sqrt{s_{NN}} = 2.76$ TeV, compared with PYTHIA Perugia 11 and JEWEL models.

physics mechanism in JEWEL model is based on the fact that soft modes are transported to large angles relative to the jet axis and this leads to a collimation of the jet.

All the ALICE jet shapes measurements show a consistent picture compatible with jets more collimated and with a harder fragmentation in Pb–Pb collisions than in pp, differently from the jet broadening and softening picture, expected from some jet quenching models.

References

[1] J. Gallicchio and M. D. Schwartz, Phys. Rev. Lett. **107** (2011) 172001
[2] A. J. Larkoski, J. Thaler and W. J. Waalewijn, JHEP **1411** (2014) 129
[3] A. Majumder and J. Putschke, Phys. Rev. C **93** (2016), 054909
[4] A. J. Larkoski, S. Marzani and J. Thaler, Phys. Rev. D **91** (2015), 111501
[5] M. Dasgupta, A. Fregoso, S. Marzani and G. P. Salam, JHEP **1309** (2013) 029
[6] A. J. Larkoski, S. Marzani, G. Soyez and J. Thaler, JHEP **1405** (2014) 146
[7] L. Cunqueiro [ALICE Collaboration], Nucl. Phys. A **956** (2016) 593
[8] M. Cacciari and G. P. Salam, Phys. Lett. B **659** (2008) 119
[9] G. Soyez, G. P. Salam, J. Kim, S. Dutta and M. Cacciari, Phys. Rev. Lett. **110** (2013), 162001
[10] P. Berta, M. Spousta, D. W. Miller and R. Leitner, JHEP **1406** (2014) 092
[11] S. Acharya *et al.* [ALICE Collaboration], arXiv:1702.00804 [nucl-ex]
[12] http://hepunx.rl.ac.uk/ adye/software/unfold/RooUnfold.html
[13] T. Sjostrand, S. Mrenna and P. Z. Skands, JHEP **0605** (2006) 026
[14] M. Bahr *et al.*, Eur. Phys. J. C **58** (2008) 639
[15] K. C. Zapp, Eur. Phys. J. C **74** (2014), 2762
[16] N. Armesto, L. Cunqueiro and C. A. Salgado, Eur. Phys. J. C **63** (2009) 679